ARCHIVES OF ELECTRICAL ENGINEERING VOL. 63(1), pp. 29-46 (2014)

DOI 10.2478/aee-2014-0003

Modal-frequency spectrum of magnetic flux density in air gap of permanent magnet motor

PAWEL WITCZAK, WITOLD KUBIAK, MARCIN LEFIK, JACEK SZULAKOWSKI

Institute of Mechatronics and Information Systems, Lodz University of Technology
ul. Stefanowskiego 18/22, 90-924 Łódź, Poland
e-mail: pwitczak@p.lodz.pl

(Received: 19.08.2013, revised: 04.10.2013)

Abstract: The classic relationships concerning the harmonic content in the air gap field of three-phase machines are presented in form of series of rotating waves. The same approach is applied to modeling of permanent magnet motors with fractional phase windings. All main reasons of non-sinusoidal shape of flux density distribution, namely, magnets' shape and their placement, slotting, magnetic saturation and eccentricity are also related to their counterparts in modal-frequency spectrum. The Fourier 2D spectrum of time-stepping finite element solution is confronted with results of measurements, with special attention paid to accuracy of both methods.

Key words: electromagnetic fields and waves permanent magnet machines, air gap magnetic flux, spectral analysis, finite element method

1. Introduction

Recently the spectrum analysis of the magnetic field in the air gap is more often taken into consideration in the design of modern electrical machines. It is related with the common use of power electronic supplies, which generate additional distortions of the time and spatial distribution of the magnetic flux density, even though the control strategies become better and better. It results in the increase of vibrations and acoustic emission, as well as eddy current loses. In case of machines with surface mounted permanent magnet excitation it can cause increase of their temperature and as the consequence, the further demagnetisation.

The harmonic analysis of magnetic field in alternating current machines is a classic problem. The main monograph is the work of Heller and Hamata [1] concerning induction motors. A lot of other dissertations in this field were published lately e.g. [2-4]. In the domain of machines with permanent magnet excitation the papers submitted by Zhu et al. [5-10] should be considered as the most important. They present the most important steps in modelling this class of machines, referred to by other authors developing the method for the use of description of particular issues, like: calculation and minimising parasitic torques [11, 14, 16, 22], taking into account flaws of assembly and supply [12, 13, 15, 19] and vibro-

acoustic effects as well [17, 20]. In small machines, more and more often, windings with fractional number of slots per pole and phase are used [21] enabling production of multi-pole motors and with concentrated windings [18], which leads to the decrease of weight.

The objective of this paper is to present a coherent calculation methodology of magnetic field flux density in the air gap of permanent magnet excited machines, utilising rotating field components of different modes and frequencies. It should be noted that this method exactly corresponds with the resulting structure obtained from a double Discrete Fourier Transform (2DFT). Apart from modification of classic formulas the results of analytical and finite element (FE) calculations were presented for consecutive stages of the analysis. The "computational noise", decreasing the accuracy of the numerical calculations, was also pointed out. The theoretical considerations were verified by measurements of the time and spatial distribution of flux density in the air gap of a machine with fractional winding in the stator. The results of measurements were presented also as 2DFT spectra. The outcome of this work enables precise determination of the reason of occurrence of a particular harmonic in the two-dimensional, time and spatial spectra of the magnetic flux density radial component in the machine's air gap.

2. Magnetic field excited by permanent magnets

The assembly of permanent magnets, placed on the rotor, plays the main part in the generation of magnetic field in the machine. Naturally the angular span of the magnets is smaller than the pole pitch, therefore the magnetic field induced in the air gap is more or less distorted from the ideal, sinusoidal shape. Firstly, let us consider an idealized case, when the magnetic field is excited by surface mounted permanent magnets in a uniform gap between cylindrical, ferromagnetic cores of the stator and rotor. Figure 1 presents the numerical calculation results of the magnetic flux density radial component distribution in the air gap, directly beside the surface of the stator. The magnet span equals to $0.8 \cdot \pi$. The different radius profiles had been complemented by a simplified rectangular distribution when the magnetic field occurs only between the magnets and the stator. The minimal mechanical gap in all cases is the same.

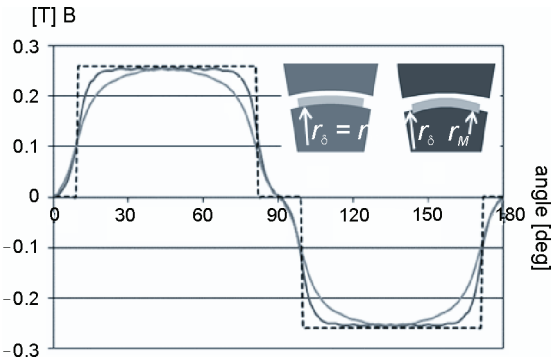

Fig. 1. Magnetic flux density radial component distribution in the machine with cylindrical core of the stator, air gap radius r_δ .and magnet radius r_M: a) $r_M = r_\delta$; b) $2r_M = r_\delta$; c) $r_M = r_\delta$, rectangular distribution

The results, as expected, gave lower values of the magnetic flux whilst the shape was closer to a sinusoid. The obtained curves, complemented anti-symmetrically to a full double pole pitch, were transformed to harmonic components. The analytical solution exists only for the simplified, rectangular case:

$$B_k = \frac{2}{\pi}\int_{\frac{\Delta}{2}}^{\pi-\frac{\Delta}{2}} B_m \sin(k\beta)d\beta = 2B_m \sin c\left(k\frac{\pi}{2}\right)\cos\left(k\frac{\Delta}{2}\right), \tag{1}$$

where B_m is the amplitude of the rectangular curve and Δ represents the angular distance between the different magnet poles. The function $\sin c(x) = \sin(x)/x$ (lat. *sinus cardinalis*) is even against its argument and is frequently used in harmonic analysis. Its single-sided curve is shown in Figure 2. As the consequence, the function given by formula (1) has non-zero values only for components with odd orders of μ.

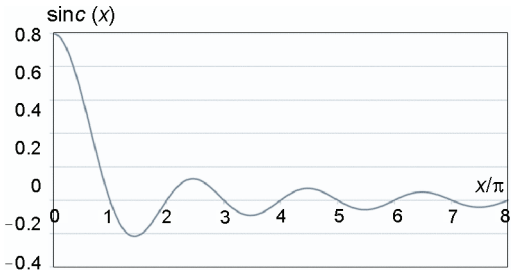

Fig. 2. Single-sided curve of sinus cardinalis

Amplitude spectrum of the rectangular curve can be described as

$$B_k = \frac{4}{\mu\pi}B_m \cos\left(k\frac{\Delta}{2}\right) \tag{2}$$

for k being a sequence of odd natural numbers. The distribution of magnetic flux density for pole pitch geometry a) and b) is also symmetrical in geometry and magnetic field distribution, as is in case c), therefore, in these cases only odd components can occur, as well. Nevertheless, the numerical computation always imply additional errors, like in this example, manifesting with the presence of non-zero amplitude values of even components. The calculation results of amplitude power spectrum (square of the RMS values) are presented in Figure 3, in logarithmic approach, according to formula:

$$L_{Bk} = 20\log\frac{B_k}{B_1} + L_{\text{noi}}, \tag{3}$$

where B_k/B_1 is the ratio of the flux density k-number harmonic to the first one and L_{noi} represents the level of "computational noise" chosen arbitrarily to suppress the dominant even harmonics. With the value of L_{noi}= 42 dB , the main even harmonic equals approximately 0.5% of the fundamental one.

The results obtained show clearly that numerical computations should be used to determine the spatial spectrum of the magnetic field in the machine's air gap. This approach helps avoiding the level of errors of about ten to twenty decibels. The magnets' profile change decreases significantly the distortion from the sinusoidal distribution, however, it reduces the amplitude of the fundamental harmonic by few percent.

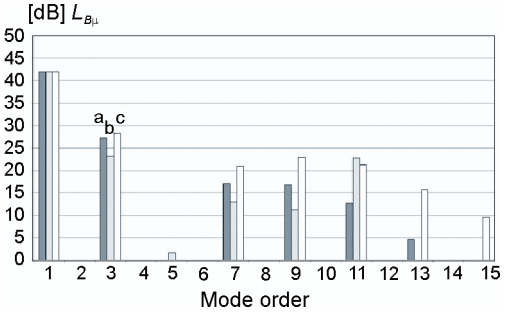

Fig. 3. Amplitude spectrum of the magnetic flux density radial component distribution in the machine's air gap, with cylindrical core of the stator and surface mounted permanent magnets – denotations as in Figure 1

The ratio $B_1(\mathrm{b})/B_1(\mathrm{a}) = 0.94$ have been obtained for the investigated geometry. Setting the position of the rotor's coordinate system 0β, so that the magnetic flux density maximum occurs at the zero point, enables presenting the radial component by the following series

$$B(\beta) = \frac{1}{2}\sum_{\mu=-\infty}^{\infty} B_k e^{jk\beta} \,. \tag{4}$$

In the further calculations it is often more convenient to use the spatial order p_k related to the full circumference of the machine

$$p_k = kp_0 \tag{5}$$

where p_0 is the number of magnet pole pairs. Introducing the coordinate system for the stator 0α, given by the formula:

$$\alpha = \beta + \Omega t, \tag{6}$$

where Ω is the rotational frequency of the rotor, the magnetic flux density field excited by the magnets can be expressed in the stator's coordinates as

$$B(\alpha, t) = \frac{1}{2}\sum_{k=-\infty}^{\infty} B_k e^{jk(p_0\alpha - \omega_0 t)}, \tag{7}$$

where ω_0 is the supply frequency. The phase velocity $\Omega_{\phi k}$ is the characteristic quantity for the wave motion of a particular harmonic, defined for the set of waves described with Equation (7) as

$$\Omega_{\phi k} \underline{\underline{\mathrm{def}}} \frac{1}{p_k}\frac{\mathrm{d}\phi}{\mathrm{d}t} = \frac{\omega_0}{p_0} = \Omega. \tag{8}$$

The constant value of the phase velocity for the set of waves of different frequencies against the stator, means the invariable shape of the resultant wave in the time domain, which in present analysis results from the assumed cylindrical geometry of the magnetic core. In case of such definition of this set, the phase velocity is equal to the, so-called, group velocity Ω_{gk}

$$\Omega_{gk} \underset{=}{\text{def}} \frac{\partial}{\partial p_k}\frac{\mathrm{d}\phi}{\mathrm{d}t} = \frac{\omega_0}{p_0} = \Omega. \tag{9}$$

Therefore, the relation between the phase velocity and order number (wave number) of the above set of rotor harmonics lays on a straight line passing through the center of the co-ordinate system on the spectral plane.

3. Magnetic field excited by symmetrical three-phase winding

The issue of rotating flux field excited by a three-phase winding is a basic knowledge problem in the domain of alternating current machines. For the convenience of the further considerations it will be presented with the same notation approach as for the field excited by the permanent magnets. Firstly, let's consider the formal case when each pole pitch has only one coil of the phase winding, with the angular stretch of $(\pi - \Delta)$. In case of a double layer winding it would be actual coils. In case of a single layer winding the actual coil can be replaced by two coils with half the number of turns. Of course, the chording Δ will be equal zero in that case. If we disregard the slot openings and the magnetic tension inside the core, the flux density field will have a rectangular distribution shape in the air gap, as in Figure 1c and its amplitude spectrum will also be described by Equation (1). If the winding (phase belt) consists of more than one coil $-q = Q_s/6p_0 > 1$ then a superposition of waves occurs. The waves are shifted by a phase angle resulting from the slot pitch multiplied by the order number of the wave considered. The amplitude approach is characterized by the group coefficient given by the classic formula

$$\xi_{qk} = \frac{\sin\left(k\frac{\pi}{6}\right)}{q\sin\left(k\frac{\pi}{6}\right)}. \tag{10}$$

Therefore, the amplitude spectrum of flux density B_k excited by a phase winding with q slots per pole and phase is equal

$$B_k = \frac{4}{k\pi} qB_m\xi_{qk}\cos\left(k\frac{\Delta}{2}\right). \tag{11}$$

Its commonly known that the resulting field in a three-phase machine is an aggregation of three fields shifted in time by an angle of $2\pi/3$, excited by windings which axes are shifted in space by geometrical angle of $2\pi/3p_0$. In a symmetrical machine, with integer number of q,

supplied with a three-phase sinusoidal current with frequency ω_0, two groups of waves are formed in the air gap. The order of the waves against the double pole pitch equals $k = 1 \pm 6n$, where n is a natural number. The combined amplitude is one and a half times greater than the amplitude of one phase component. The time and spatial form is characterized by the equation

$$B_k(\alpha,t) = \frac{6}{k\pi} qB_m \xi_{qk} \cos\left(k\frac{\Delta}{2}\right) e^{1(p_k\alpha-\omega_0 t)}. \tag{12}$$

In can be noticed that in case of $k > 0$ the wave rotates forward with the rotation direction of the rotor and in case of $k < 0$ the wave rotates backward. All components excited by permanent magnets on the rotor, of course, must rotate forward – see (7). Figure 4 shows the spectrum structure of flux density field in the air gap of a synchronous machine

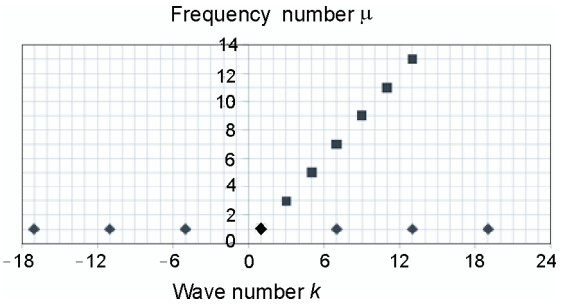

Fig. 4. The two-dimensional amplitude spectrum structure of magnetic flux density radial component in a smooth air gap of a synchronous machine, with integer q and mono-harmonic phase currents: ■ – field component excited by permanent magnets; ◆ – field component excited by three-phase winding

If a slot skew is introduced against the rotation axis, or other equivalent angular shift of the rotor's magnets, then the averaged, in this way, amplitude of the circumferential harmonic is decreased by multiplying the result of (12) by the so called skew coefficient ξ_k, calculated [21] from equation

$$\xi_{sk} = \left|\sin c\left(p_k \frac{\alpha_{sk}}{2}\right)\right|, \tag{13}$$

α_{sk} means the skew angle counted, in radians, between the terminal planes of the uniformly twisted stator or rotor core stack, referred to the full circumference of a motor.

4. Magnetic field excited by non-symmetrical three-phase winding

In the case of windings with non-integer number of slots per pole and phase it is not profitable to seek analytical solutions of the spatial spectrum of flux density – the formulas would be too complicated. In the each particular case a classic analysis of magnetic field distribution in the air gap should be carried out, for elementary coils in an individual phase band. The algorithm of the procedure may be as follows:

- extract the smallest, repeatable fragment of the phase winding – so called belt;
- determine the spatial distribution of magnetic flux density in the air gap excited by singular coils, then using the superposition calculate the resultant field;
- determine the Fourier Transform (spectrum) of obtained function.

As an example let us consider a single-layer winding with $q = 3/2$ resulting from a three-phase stator with slot number $Q_s = 36$ and $p_0 = 4$. It can be noticed that the structure repeats itself each 18 slots – the phase windings have two belts, each consisting of three coils. The scheme of phase coils is presented in Figure 5.

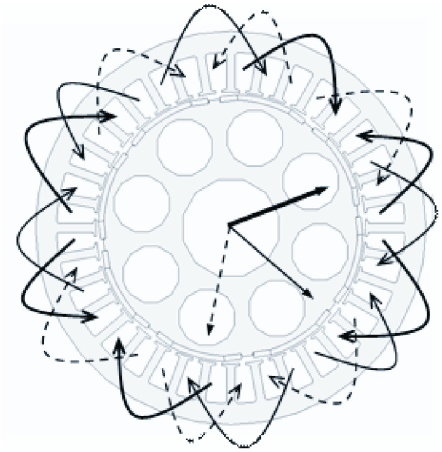

Fig. 5. Connection scheme of three-phase, single layer winding: $Q_s = 36$, $p_0 = 4$ and $q = 3/2$ with magnetic axes of phase belts

Indicating the number of slots assigned to the winding belt by Q_p – in this case $Q_p = 18$, the distribution of flux density excited by a singular coil can be calculated. The magnetic flux Φ in the air gap having width δ and unitary dimension along the rotation axis, produced by a coil y-wide, conducting a flow of ampere-turns ϑ_m is equal

$$\Phi(t) = \mu_0 \frac{\vartheta_m}{\delta\left(\frac{1}{y} + \frac{1}{Q_p - y}\right)} e^{j\omega t}. \tag{14}$$

The flux density in the air gap, in the area under the investigated coil equates

$$B_{\text{in}}(t) = +\frac{\mu_0}{\delta}\vartheta_m \frac{Q_p - y}{Q_p} e^{j\omega t} \tag{15}$$

and in the remaining part of the air gap

$$B_{\text{out}}(t) = -\frac{\mu_0}{\delta}\vartheta_m \frac{y}{Q_p} e^{j\omega t}. \tag{16}$$

Adding the contributions of all coils in the belt an oscillating field is obtained. Its distribution along the belt, for the analyzed machine, at time when the current reaches maximum, is depicted in Figure 6. That spatial distribution generates the amplitude spectrum also presented in this figure. The order k of the belt's spectrum (referred to the double pole pitch) is equal, in this case

$$k = \frac{v}{2}. \tag{17}$$

The spatial asymmetry of the coils in the winding belts, in case of $q = 3/2$, is the reason of generating harmonics with the "half" orders k – while referred to the whole circumference the orders kp_0 are integer, of course. In other circumstances the no-source condition of the magnetic field in the machine would not be fulfilled.

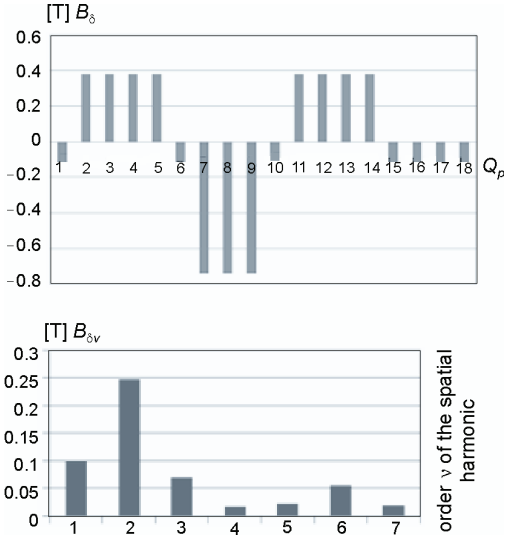

Fig. 6. Flux density distribution in the air gap of the machine produced by the winding belt: δ = 1.0 mm, Q_p = 18, $p_0 = 4$ and the slot current magnitude ϑ_m = 200 ampere-turns accompanied with its amplitude spectrum (order related to the belt angular size)

The magnetic axes of the phase belts are shifted by 6 slots, as shown in Figure 5, which corresponds to a spatial phase shift for the fundamental harmonic (of order $k = 1$ or $v = 2$) $\phi_0 = 4\pi/3$, because the period of this component equals $Q_s/p_0 = 9$ slots. However, it is better to perform the spectral analysis in the coordinate system referred to the span of the winding belt that means with the indicators v. In that case the phase angle of the subsequent spatial harmonics is equal

$$\phi_v = \pm v\frac{2\pi}{3}. \tag{18}$$

Equation (18) means that in case of supplying all windings with sinusoidal in time currents, shifted in phase, according to the chosen winding, by $\pm 2\pi/3$ radians, the resulting field of the harmonics with the order $v = 3, 6, 9...$ will be equal zero. Proceeding in the same way as in case of a machine with integer number of q, we acquire a set of harmonics with the orders $\nu = 1 \pm 3n$, where n is a natural number. The function equation describing the components of flux density waves, referred to the whole circumference of the machine, has a form of

$$B_v(\alpha, t) = B_v\, e^{j\left(\frac{v}{2}p_0\alpha - \omega_0 t\right)}. \tag{19}$$

The structure of the two-dimensional spectrum of magnetic flux density in the air gap of a machine with q = 3/2 is shown in Figure 7. Comparing it with the spectrum of a machine with an integer number of q, presented in Figure 4, it can be noticed that the density (number) of the component harmonics, produced by the stator currents, is twice as big. The phase angle in time of the flux density harmonics in the air gap is usually described in the range (−π, +π). That means the phase velocity $\Omega_{\phi\nu}$ (8) is the same, as for the modulus, for all components of the spectrum and it equals

$$\Omega_{\phi\nu} = \pm\Omega \tag{20}$$

The instantaneous value of the phase angle ϕ_ν, for a chosen harmonic component of the flux density in the air gap, will therefore equate

$$\phi_\nu = \pm\Omega t + \phi_{\nu 0}, \tag{21}$$

where the constant $\phi_{\nu 0}$ depends on the choice of the time and place of observation. Replacing time with the instantaneous angular position β_0 of the rotor, with the number of pole pairs p_0, we obtain

$$\phi_\nu = \pm\Omega\frac{p_0}{\Omega}\beta_0 + \phi_{\nu 0} = \pm p_0\beta_0 + \phi_{\nu 0}, \tag{22}$$

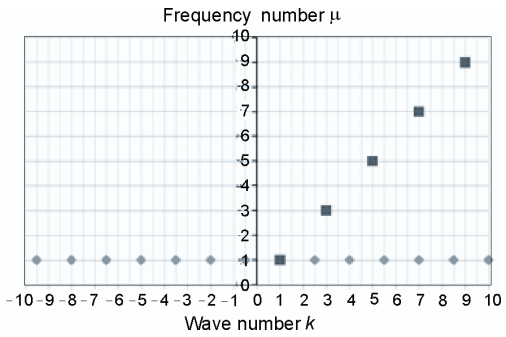

Fig. 7. The two-dimensional amplitude spectrum structure of magnetic flux density radial component in a smooth air gap of a synchronous machine, with q = 3/2 and monoharmonic phase currents: ■ – field component excited by permanent magnets; ◆ – field component excited by three-phase winding

The parallelism of functions $\phi_\nu(\beta_0)$ does not mean that the components of the spectrum are stationary against each other for the same phase velocity (counted each time in the range −π, +π). Quite opposite, for the investigated winding structure with $q = {}^3/_2$, the displacement e.g. of the maximums of consecutive components, measured with the geometrical angle β_ν is given by equation

$$\beta_\nu = \frac{\phi_\nu}{\mu\, p_0} = \pm\frac{2}{\nu}\beta_0. \tag{23}$$

Examples of spatial distribution of magnetic flux density in the air gap, resulting from the superposition of the fundamental component in the investigated machine of the order $p_0 = 2\nu_0$

= 4 with some chosen harmonics generated by the rotor field, are presented in Figure 8. Two time instants are depicted, for which the phase shift $\Delta\omega t$ equals $\pi/2$.

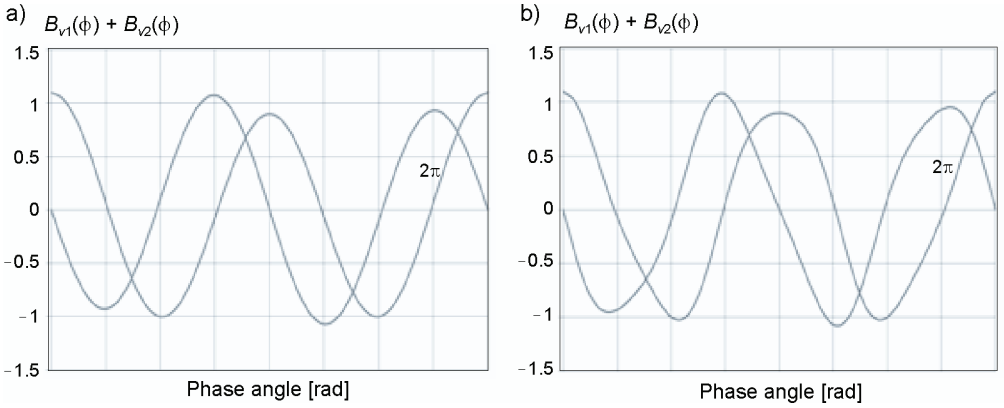

Fig. 8. Modulation of the resulting spatial distribution of magnetic flux density in the air gap by components of the same frequency and amplitude ratio $A_1/A_2 = 10$, for two different time instants $\Delta\omega t = \pi/2$ apart: a) $v_1 = +2$, $v_2 = -1$; b) $v_1 = +2$, $v_2 = +4$

5. Influence of air gap non-uniformity on the mode-frequency flux density spectrum

In the most of electric machines the air gap is not uniform. The presence of slotting, rotor eccentricity and saturation of the magnetic core causes that the permeance of the air gap, in the radial direction, changes periodically along the circumference of the machine. The lack of ferromagnetic material, real – due to cut out slots or imaginary – due to saturation, causes, that for a given magnetomotive force the flux of a particular harmonic component decreases. This effect can be estimated using classic Carter's k_c and saturation k_{ns} coefficients. Apart from that, the shape of the field in space changes, introducing additional modulation of the rotating wave of flux density, associated with the period of geometry disturbance.

In case of slotting, the magnetic permeance of the air gap changes periodically Qs times per one circumvolution. The rotating ampere-turns flow (originating from the rotor or stator) acting with the alternating air gap permeance generates additional flux density waves characterized by the equation

$$B_{uk}(t,\alpha) = \left[\frac{1}{k_C} + \gamma_1 \cos(Q_s\alpha) + \gamma_2 \cos(2Q_s\alpha) + \ldots\right] B_k e^{j(p_k\alpha - \omega_\mu t)}, \tag{24}$$

where the series of coefficients γ_i results from the spatial harmonic transformation of the actual permeance and k_c is the Carter's coefficient. Their values, invoked for reader's convenience below, might be estimated using equations contributed by Heller and Hamata [1], which in case of a rather big air gap in synchronous machines give the following dependencies

$$\gamma_n = 0.07\frac{b_4}{\delta}\frac{4}{n\pi}\left[\frac{1}{2}+\frac{\left(n\frac{b_4}{t_Q}\right)^2}{0.78-2n\frac{b_4}{t_Q}}\right]\sin\left(1.6n\pi\frac{b_4}{t_Q}\right) \tag{25}$$

where the quantities b_4, t_Q, δ represent accordingly: slot opening, slot pitch and mechanical air gap dimension. The Carter's coefficient equals

$$k_C = \frac{1}{1-0.11\frac{b_4^2}{\delta t_Q}}. \tag{26}$$

For the actual data: $b_4 = 3$ mm, $t_Q = 12$ mm, $\delta = 1$ mm; the coefficients equal: $\gamma_1 = 0.15$, $\gamma_2 = 0.10$, $\gamma_3 = 0.05$ and $k_c = 1.09$. Replacing the trigonometric functions with exponential expressions and using notation $\cos\alpha = 0.5\exp(\pm j\alpha)$, we obtain

$$B_{uk}(t,\alpha) = \left[\frac{1}{k_C}+0.5\gamma_1 e^{\pm jQ_s\alpha}+0.5\gamma_2 e^{\pm j2Q_s\alpha}+\ldots\right]B_k e^{j(p_k\alpha-\omega_\mu t)}. \tag{27}$$

The application of formula (27) causes that the amplitude of the wave in a one-side slotted air gap will be reduced k_c times and deformed by additional harmonics. On the spectral plane in the coordinates (k, μ) – as referred to double pole pitch or $(p_0 k, \mu)$ if referred to the whole circumference of the machine, there will be a double sided series of "neighbour" spatial harmonic components with coordinates $(k \pm nQ_s/p_0, \mu)$ or $(p_0 k \pm nQ_s, \mu)$. It should be noted that the positions of additional components, related to the slotting and produced by the reaction of the stator currents, coincide with the harmonics already generated by the placement of the winding coils in the machine. Therefore only the amplitude of these components is modified.

By analogy the influence of the saturation can be determined. Assuming that the field excited by the assembly of permanent magnets in the rotor decide about the value of magnetic permeability in the magnetic core, we receive a collection of disturbances of the uniformity of magnetic tensions rotating against the stator with the rotational frequency $\Omega = \omega_0/p_0$, having doubled frequency in space and time – the magnetic permeability depends on the modulus of flux density. The set of these harmonics will have the same group velocity, on the spectral plane, as the rotor's field – the inclination of the straight line $\mu(p_\mu)$ is equal $1/p_0$ and will contain the source component

$$B_{sk}(\alpha,t) = \frac{1}{k_{ns}}\left[1+\sum_s 0.5\sigma_S e^{j2s(p_0\alpha-\omega_0 t)}\right]B_k e^{j(p_k\alpha-\omega_\mu t)}. \tag{28}$$

The sequence of numbers s, as explained while presenting the rotor structure, contains only odd natural numbers. The intensity of disturbances σ_s has not good analytical estimations – examples of numerical calculation results are presented further in this paper.

The evaluation of the effect of rotor's static eccentricity on the flux density field shape in the air gap is based on the function approximating the variation of air gap dimension

$$\delta(\alpha) \cong \delta\left[1 + 0.5\varepsilon e^{\pm j\alpha}\right], \tag{29}$$

where ε is the dislocation of the rotor's symmetry axis against the stator axis, divided by the dimension of the air gap. If the eccentricity is so small that it can be assumed $\varepsilon^2 \ll 1$, then its presence should only give a specific "dissolution" of the original spectrum component. For all rotating component waves of the stator's or rotor's flux density we acquire additional waves differing from the original wave $B_k(\alpha, t)$ by the order ±1.

$$B_{\varepsilon k}(t,\alpha) = \left[1 + 0.5\varepsilon e^{\pm j\alpha}\right] B_k e^{j(p_k\alpha - \omega_\mu t)}. \tag{30}$$

regarding to the whole circumference of the machine. Referring the order of these waves to the double pole pitch once again we receive "fractional" harmonics ($k \pm 1/p_0$).

The positions of the spectrum components caused by the slotting, saturation and eccentricity are presented schematically in Figure 10. It was assumed, for this diagram, that the harmonics generated by the three-phase winding would have the order indicator k (referred to the double pole pitch) in the range of (−9.5 to +14). Additionally the so-called "secondary" harmonics – e.g. produced by the stator's field, eccentricity and saturation, are disregarded. It should be noted that the depicted positions, assigned to components connected with a particular physical phenomena does not mean that they will have a substantial magnitude in the considered machine.

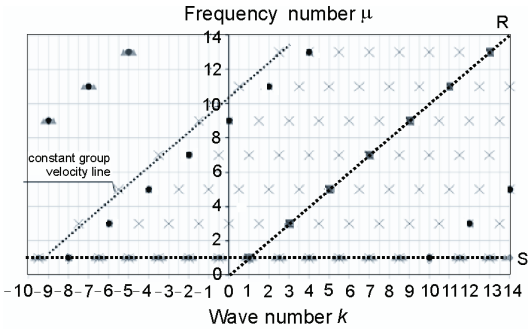

Fig. 9. The two-dimensional amplitude spectrum structure of magnetic flux density radial component in a single side slotted air gap of a synchronous machine, with q = 3/2 and mono-harmonic phase currents: ■ – field component excited by permanent magnets (R) – non-dispersive wave; ◆ – field component excited by three-phase winding (S); ● – field component excited by stator's slotting; ▲ – field component excited by eccentricity; × – field component excited by saturation

The amplitude of any particular component and whether it is greater than the computational or measurement background noise depends on many of factors discussed earlier. The fact that a component with a coordinate $k = 0$ exists, which means a homopolar flux, should be also commented. This flux may occur in a machine but its amplitude cannot be determined in the simplified, two-dimensional model of the magnetic field utilised in this paper.

6. Numerical analysis of the magnetic field in machine air gap

The calculations of the time spatial distribution of flux density in the two-dimensional cross-section of the machine were made with the time stepping technique for a magnetostatic

problem, at rated load conditions. In the each time step the rotor and the resultant stator's field was turned systematically by an angle $\Delta\alpha_{geo} = 2\pi/\mathrm{N}$, where $N = 360$, in the range of the double pole pitch. It was assumed that the phase currents, supplying the windings, were sinusoidal in time. An example of the distribution of magnetic flux in the analysed eight pole machine and the radial component in the air gap are presented in Figure 11. The occurrence of the second order component of magnetic field can be easily noticed – observing the shape of the flux in the rotor or comparing the consecutive, negative amplitudes of the flux density distribution.

The flux distribution in the air gap was sampled in N points evenly spread over the whole circumference, directly under the surface of the stator. The resulting matrix $B_r(n\Delta\alpha, m\Delta t)$, $m = 1... N/p_0$, $n = 1... N$ was converted with the two-dimensional Fourier Transform, centered and transposed to a one-sided form.

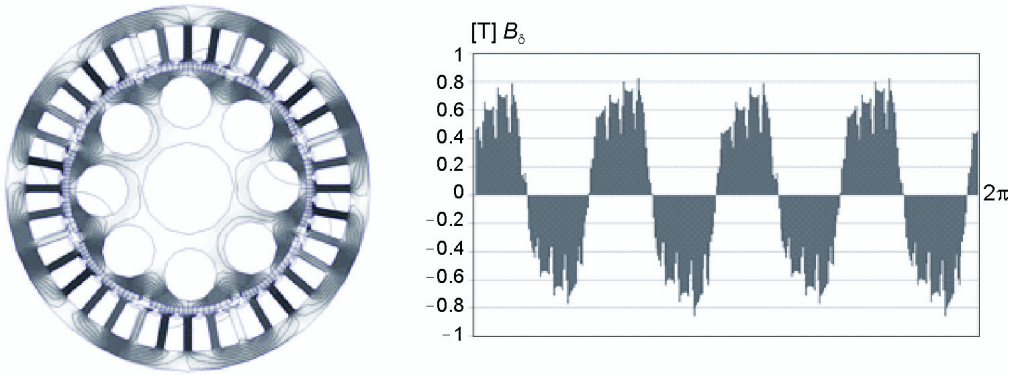

Fig. 10. Instantaneous distribution of magnetic flux and magnetic flux density radial component B_δ distribution in the air gap of a synchronous machine, with $p_0 = 4$, $q = {}^3/_2$, at rated load conditions

The cited parameters of the computational process lead to the following boundary values of Nyquist's angular velocity ω_{Ny} and wave number p_{Ny} for a two-dimensional spectrum

$$\omega_{Ny} = \frac{N}{2p_0}\omega_0 = 45\omega_0$$
$$p_{Ny} = \frac{N}{2} = 180. \tag{31}$$

It should be noted that the static analysis of the magnetic field distribution enables, as first, the application of the one-sided form of the amplitude spectrum – the 2DFT matrix is anti-symmetrical, and secondly, the choice any value of the ω_0, since there are no eddy currents. The calculations were performed for two conditions – for a co-axially positioned rotor and with a static eccentricity of $\varepsilon = 0.15$. The resulting modal-frequency spectra are compiled in Figure 11. Limiting the range of the presented calculation results improves the legibility and enables easy comparison with the measurement results supplied further.

The spatial range of the measurements was limited due to the number of probes $-p_{Ny}$ was equal $Q_s/2 = 18$. The logarithmic scale of the power level of the flux density field was used because of the large amplitude span between the various components, the reference value of flux density $B_{\text{ref}} = 1$ T.

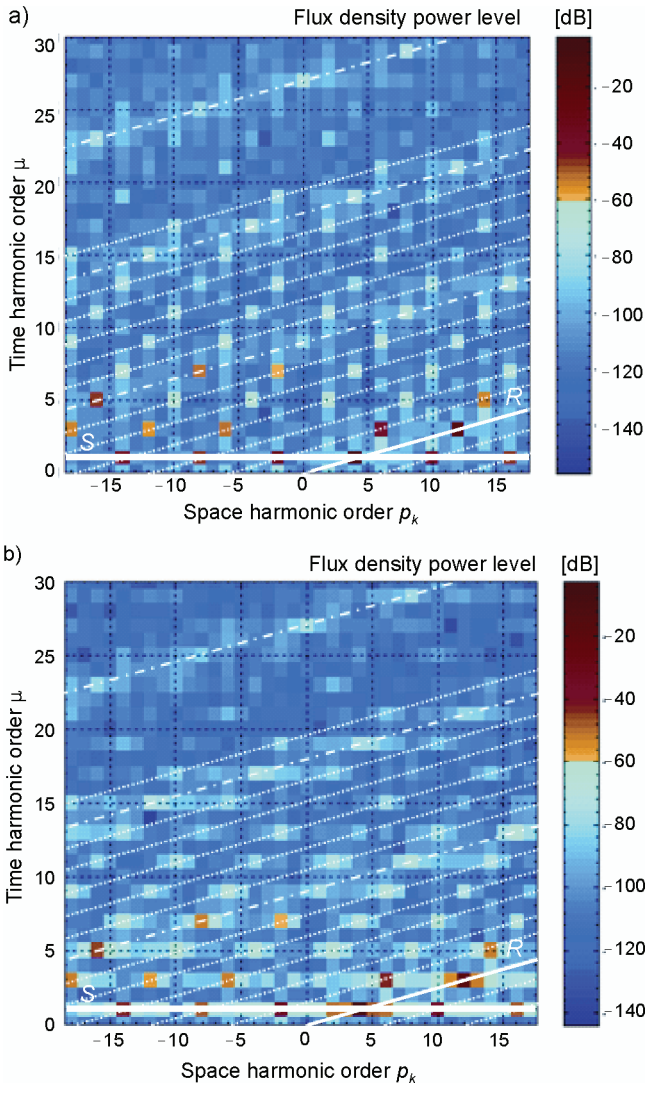

Fig. 11. Modal-frequency amplitude spectra of the flux density power level for the magnetic flux density radial component distribution in the air gap of a synchronous machine, with $p_0 = 4$, $q = 3/2$, at rated load conditions, FE computations: a) centered rotor , b) static eccentricity $\varepsilon = 0.15$. —— rotor (R) and stator (S) harmonics, -·-·- slotting harmonics, ···· saturation harmonics

$$L_B(k,\mu) = 20\log\frac{B(k,\mu)}{B_{ref}}. \tag{32}$$

As previously $p_k = kp_0$ is the space harmonic order referred to machine circumference and μ is the frequency order. Additionally a nonlinear color scale was applied, emphasizing the components with the amplitude greater than 1 mT. The computational error in form of the even harmonics may be also observed.

Evaluating the results obtained it can be noticed, that an interpretation of the origin of all harmonics has been given, both in case of eccentricity and its lack. In case of eccentricity the "dissolution" of the dominant harmonics was larger by one than the assumption in the simplified formula (30). Taking into account the actual slot skew and applying Equation (13) decreased the amplitudes of the consecutive spatial harmonics, however, presenting the difference in the scale of Figure11 would be unnoticed.

7. Experimental verification of the air gap flux density distribution in time and space

The analyzed machine with $p_0 = 4$, $q = 3/2$, was equipped with coil probes on the each tooth tip of the stator. The matrix of 36 time signals of the measured average flux density, at the rated load condition, was converted with the Discrete Fourier Transform, in the same way as the finite elements method computational results. The diagram is presented in Figure 12.

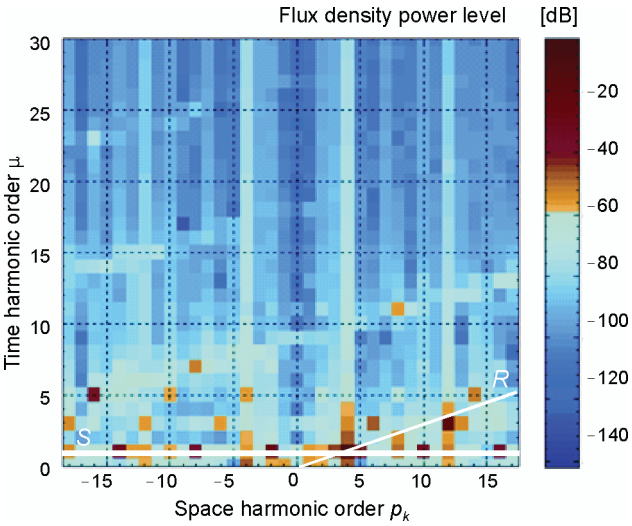

Fig. 12. Modal-frequency amplitude spectra of the flux density power level for the magnetic flux density radial component distribution in the air gap of a synchronous machine, at rated load conditions, measurements —— rotor (R) and stator (S) harmonics, -·-·- slotting harmonics, ··· saturation harmonics

The same lines were marked, as in Figure 11, of the harmonic attachment to the set generated by the reaction between the source harmonic and the rotating field of the magnets. Comparing it with the theoretical determinations, still a good agreement can be noticed between the structure of the experimental spectrum and its assumed shape. The most significant differences are: a greater contribution of the eccentricity in the measured spectrum – the fundamental time harmonic line ($\mu = 1$, p_k) is almost entirely filled and the presence of even time harmonics,

possibly the result of bending vibrations in reaction with the flux density and/or not exactly adjusted acquisition time to supply frequency. The distinct vertical harmonic sets with the same spatial order and continuous spectrum in time are caused by the non-simultaneous acquisition of data in some of the measurement channels, even though some approximated compensation of the phase shift was introduced a'posteriori in measured signals. They are still visible although their power levels are about −45 to −60 dB. The harmonics related to the slotting of the stator appear at the power levels from −4 to −70 dB. The measured spectra contain quite high harmonic components constant in time, with amplitude for the fundamental harmonic approximately 20 mT ($L_B \cong -40$ dB) and for higher order spatial harmonics typically, about 5 mT ($L_B \cong -46$ dB). It can be caused by the varying coupling of the measurement coils with the leakage flux in the slot openings, due to high saturation in the tooth tips.

Comparison of the theoretical computations for the simplified model (Fig. 1) and the whole cross-section of the motor (Fig. 10) with the measurement results are brought together in Table 1. The estimated precision of quantities concerns the constant value in time or even time harmonics. The significant differences in the error estimations between the theoretical and experimental results arise from the spatial resolution – in the space taken by one measurement coil (one slot pitch), there are almost 30 nodes of the finite element mesh.

Table 1. Calculated and measured amplitudes [T] of radial flux density harmonics in air gap at rated load conditions

Order (p_k, μ)	(−14, 1)	(−8, 1)	(−2, 1)	(4, 1)	(10, 1)	(12, 3)
FE full model (±0.002 T)	0.009	0.005	0.045	0.720	0.014	0.110
FE simplified model (±0.004 T)	0.015	0.035	0.095	0.704	0.022	–
Measurement (±0.010 T)	0.020	0.015	0.072	0.739	0.029	0.105

Additional confirmation of the correctness of the carried out reasoning can be obtained by analyzing the change of the phase shift of individual components as the function of the shaft rotation angle β_0, presented in Figure 13.

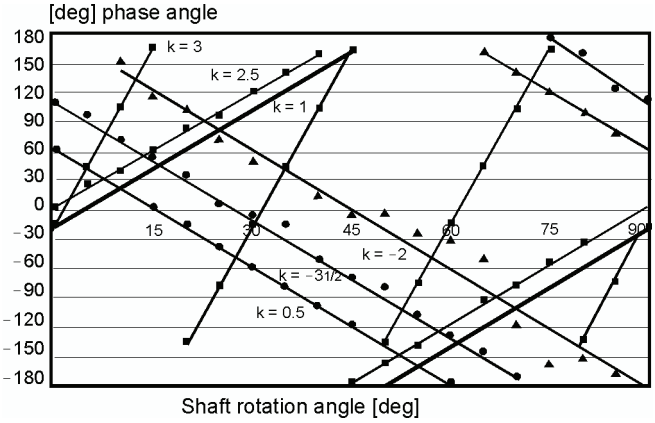

Fig. 13. Functions of phase shifts of the flux density harmonics measured in the air gap of a synchronous machine, with $Q_s = 36$, $p = 4$ (order k referred to double pole pitch)

A good conformity of the phase function inclinations with the equation (23) can be observed, as well as the term of synchronism $k = 0.5(-1 + 3n)$ or anti-synchronism $k = 0.5(-1 - 3n)$. The exception is the function for component of wave number $k = 3$, which cannot be produced by the three phase winding. Its inclination is here three times greater than that one for the fundamental component $k = 1$. It means the same phase velocity as for the fundamental component – see (8), so it was generated by the rotor's magnets.

8. Summary

The analytical dependencies derived in this paper, coupling the spatial and time orders with the topology of the stator, magnet assembly shape and the level of saturation, enable a precise determination of the reasons of generating higher time harmonics of the flux density field in the machine's air gap. In the investigated case, the dominant cause of the stator's slotting was ascertained, together with the saturation of the magnetic core. It was noticed, that in case of semi-closed slots, the second and third order spatial harmonics play a significant part. Usually they are ignored in the analysis. Nevertheless, concerning the importance of those analytical formulas, it is necessary to apply numerical computational methods in the machine designing process, since it is the only way to obtain accuracy of about 1%, which is required for magnetic vibration and noise or additional eddy current analysis.

References

[1] Heller B., Hamata V., *Harmonic Effects in Induction Machines.* Elsevier (1997).
[2] Bialik J., *Vibrations and electromagnetic forces in two-speed large power induction motors.* Ph. D. dissertation, Tech. Univ. of Wroclaw (2007) (in Polish).
[3] Karkosinski D., *Vibration and acoustic effects in induction cage motors.* D. Sc. dissertation, Tech. Univ. of Gdansk (2006) (in Polish).
[4] Vandevelde L., Gyselinck J., Melkebeek J., *Electromechanical analysis of vibrations and noise of squirrel cage induction motors.* Proc. of Int. Conf. on Electric Machines, Istanbul 1: 496-551 (1998).
[5] Zhu Z.Q., Howe D., Bolte E., Ackerman B., *Instantaneous magnetic field distribution in brushless permanent magnet DC motors. Part I: open-circuit field.* IEEE Trans. Magnetics 29(1): 124-135 (1993).
[6] Zhu Z.Q., Howe D., *Instantaneous magnetic field distribution in brushless permanent magnet DC motors. Part II: armature reaction field.* IEEE Trans. on Magnetics 29(1): 136-142 (1993).
[7] Zhu Z.Q., Howe D., *Instantaneous magnetic field distribution in brushless permanent magnet DC motors. Part III: effect of stator slotting.* IEEE Trans. on Magnetics 29(1): 143-151 (1993).
[8] Zhu Z.Q., Howe D., Bolte E., Ackerman B., *Instantaneous magnetic field distribution in brushless permanent magnet DC motors, Part IV: magnetic field on load.* IEEE Trans. on Magnetics 29(1): 152-159 (1993).
[9] Zhu Z.Q., Howe D., *Influence of design parameters on cogging torque in permanent magnet machines.* IEEE Trans. Energy Convers 15(4): 407-412 (2000).
[10] Zhu Z.Q., Xia Z.P., *Comparison of Halbach magnetized brushless machines based on discrete magnet segments or a single ring magnet.* IEEE Trans. on Magnetics 38(5) (2002).
[11] Hwang S.-M., Eom J.-B., Hwang G.-B. et al., *Cogging torque and acoustic noise reduction in permanent magnet motors by teeth pairing*, IEEE Trans. on Magnetics 36(5): 3144-3146 (2000).

[12] Kim T.-K., Kim S.-K., Hwang S.-M. et al., *Comparison of magnetic forces for IPM and SPM motor with rotor eccentricity*. IEEE Trans. on Magnetics 37(5): 3448-3451 (2001).
[13] Mi-Jung Kim, Byong-Kuk Kim, Ji-Woo Moon et al., *Analysis of Inverter-Fed Squirrel-Cage Induction Motor During Eccentric Rotor Motion Using FEM,* IEEE Trans. on Magnetics. 44(6): 1538-1541 (2008).
[14] Ping Jin, Shuhua Fang, Heyun Lin et al., *Analytical Magnetic Field Analysis and Prediction of Cogging Force and Torque of a Linear and Rotary Permanent Magnet Actuator*. IEEE Trans. on Magnetics 47: 3004-3007 (2011).
[15] Kawase Y., Mimura N., Ida K., *3-D electromagnetic force analysis of effects of off-center of rotor in interior permanent magnet synchronous motor*, IEEE Trans. on Magnetics 36(4): 1858-1862 (2000).
[16] Łukaniszyn M., Jagieła M., Wróbel R., *Optimization of Permanent Magnet Shape for minimum cogging torque using genetic algorithm.* IEEE Trans.on Magnetics 40(2): 1228-1231 (2004).
[17] Wach P., *Fractional windings in AC electric machines (in Polish),* PWN, Warszawa (1997).
[18] El-Refaie A.M., Jahns T.M., Novotny D.W., *Analysis of Surface Permanent Magnet Machines with Fractional-Slot Concentrated Windings.* IEEE Trans. on Energy Conversion 21(1): 34-43 (2006).
[19] Wenxiang Zhao, Ming Cheng, Wei Hua et al., *Back-EMF Harmonic Analysis and Fault-Tolerant Control of Flux-Switching Permanent-Magnet Machine with Redundancy.* IEEE Trans. on Industrial Electronics 58(5): 1926-1935 (2011).
[20] Witczak P., Wawrzyniak B., *Spectral Analysis of permanent magnet electric machines.* COMPEL 27(4): 919-928 (2008).
[21] Witczak P., *Vibration and acoustics of electric machines with permanent magnets.* Monografie Politechniki Łódzkiej, (in Polish) (2012).
[22] Gasparin L., Fiser R., *Cogging Torque Sensitivity to Permanent Magnet Tolerance Combinations.* Archives of Electrical Engineering 62(3): 449-469 (2013).